

## Supporting Online Material

A muscle-specific microRNA impedes ALS pathogenesis and promotes regeneration of neuromuscular synapses

Williams et al.

### Materials and methods

**Generation of miR-206 mutant mice.** The 2.7-kb 5' arm was amplified from 129SvEv genomic DNA and digested with Sac II and Not I and ligated into pGKNeo-F2L2DTA targeting vector. The 2.1-kb 3' arm was digested with Hind III and Eco RV and ligated between the neomycin resistance and DTA cassettes of the targeting vector. Targeted ES-cells were identified by Southern blotting with 5' and 3' external probes. One clone with a properly targeted miR-206 allele was used for injection into 3.5 day C57BL/6 blastocysts and the resulting chimeras were bred to C57BL/6 females for germline transmission. All breedings were performed in the 129SvEv and C57BL/6 mixed backgrounds. Sequences of the primers are in Table S1.

**Generation of HDAC4 mutant mice.** Mice with loxP sites flanking exon 6 of the *Hdac4* gene have been previously described and will be described in detail elsewhere (1). These mice were bred to mice expressing Cre recombinase under control of the muscle-specific *myogenin* promoter and *Mef2c* enhancer to delete HDAC4 specifically in skeletal muscle (2). All breedings were performed in the 129SvEv and C57BL/6 mixed backgrounds.

**G93A-SOD1 mice.** Transgenic mice expressing the low copy number human G93A-SOD1 mutation (B6SJL-TgNSOD1-G93A; 1Gurd1 JR2300) were obtained from Dr. Jeffrey L. Elliott. For survival analysis, miR-206<sup>-/-</sup>; G93A-SOD1 were compared to miR-206<sup>+/-</sup>; G93A-SOD1 littermates. The experiment was stopped when paralysis was so severe that the animal could not right itself.

**RNA analyses.** Total RNA was isolated from tissues using TRIzol Reagent (Invitrogen) according to the manufacturer's instructions. Northern blots to detect miRNAs generally used 8-10 µg of total RNA and were run on 20% denaturing acrylamide gels.

Oligonucleotide probes antisense to the mature miRNA were generated using the Starfire Labeling Kit (IDT). A Starfire oligonucleotide probe for U6 was used as a loading control. MiR-206 expression was quantified by densitometry and normalized to U6 expression using ImageQuant 5.0 software. Sequences of the probes are in Table S1.

RNA was treated with Turbo DNase (Ambion) prior to reverse transcription. RT-PCR with random hexamer primers was performed on RNA samples using Superscript III (Invitrogen). Quantitative real time PCR was performed using Taqman probes or SYBR Green primers. mRNA levels of the genes of interest were normalized to *Gapdh* mRNA levels. Sequences of the primers are in Table S1.

For synapse enrichment studies, the diaphragms from thy1-YFP transgenic mice were isolated (3). The endplate band, delineated by the YFP rich nerve terminals, was separated. RNA was extracted from synapse-rich and synapse-free regions using TRIzol. Quantitative real time PCR was used to assess miR-206 levels using primers specific for

miR-206 and primers for miR-206 and 7H4. *Gapdh* mRNA levels were used as a loading control. Three diaphragms were examined and each quantitative real time PCR experiment was done in triplicate. Sequences of the primers are in Table S1.

For miRNA microarray, total RNA was extracted from tibialis anterior (TA) muscles of wild-type and symptomatic G93A-SOD1 transgenic mice, and used for miRNA microarray analysis at LC Science (Houston, TX).

**Generation and analysis of lacZ reporter mice.** An 837 bp genomic fragment upstream of the *miR-206* gene (from -1576 to -739) containing conserved E-boxes was fused to the hsp68 basal promoter upstream of a lacZ reporter gene. Mutations were introduced into the three conserved E-boxes using QuikChange II Site-Directed Mutagenesis Kit (Stratagene). LacZ reporter transgenes were injected into the pronuclei of fertilized oocytes by standard techniques. Muscles of P10 transgenic mice were denervated for 10 days by sciatic nerve transection followed by staining for  $\beta$ -galactosidase activity (4). Two independent transgenic wild-type (WT) and mutant (Mt) lines were examined.

**Surgical procedures.** Surgical procedures were performed on anaesthetized 6- to 12-week old mice. Denervation was performed by cutting the left sciatic nerve in the mid-thigh region. Nerve crush was performed by crushing the sciatic nerve for 15 or 30 seconds and analyses were performed 7 and 18 days later. All animal protocols and procedures in this study were reviewed and approved by the UT Southwestern Institutional Animal Care and Use Committee.

**Plasmids and transfection assays.** The 1100 bp genomic fragment containing the miR-206 coding sequence was ligated into the pCMV6 expression vector. A 1200 bp genomic fragment of the mouse *Hdac4* 3' UTR containing the miR-206 predicted binding sites was ligated into luciferase reporter pMIR-REPORT (Ambion). Mutations in the miR-206 predicted binding sites were introduced using QuikChange II Site-Directed Mutagenesis Kit (Stratagene). Increasing amounts of the miR-206 expression vector were co-transfected with the HDAC4-UTR luciferase vector and CMV-LacZ vector. Assays were performed in triplicate and luciferase activity was determined 40 hours later and normalized to lacZ activity. The 837 bp miR-206 denervation response element was ligated into the luciferase reporter pGL3 containing a minimal hsp70 TATA element. Increasing amounts of pcDNA-MyoD (0ng, 25ng, 50ng, 100ng) were co-transfected with miR-206-enhancer luciferase vector and CMV-LacZ vector. Luciferase activity was determined 40 hours later and normalized to lacZ activity.

Small interfering RNA were designed against FGFBP1 and cloned into pcDNA 6.2-GW/EmGFP-miR (Invitrogen). To confirm FGFBP1 knockdown, a FGFBP1-mCherry construct was co-transfected with shRNAs targeting LacZ (Invitrogen) or FGFBP1 in HEK293 cells. Knockdown was determined by assessing co-expression of GFP, which marks shRNA expressing cells, and FGFBP1-mCherry. Sequences of the oligonucleotides are in Table S1.

**Gel shift assay.** Oligonucleotides corresponding to the conserved E-boxes and mutated binding sites were synthesized (IDT). Annealed oligonucleotides were labeled with <sup>32</sup>P-

dCTP using Klenow. Whole-cell lysates from COS1 cells transfected with pcDNA-myc-MyoD and pcDNA-E12 or empty vector pcDNA were isolated and used in DNA binding assays. Unlabeled oligonucleotides were used as competitors. Sequences of the oligonucleotides are in Table S1.

**Western blot analysis.** Protein lysates were resolved on 12% SDS-PAGE gels using standard procedures. Antibodies against HDAC4 (H-92 Santa Cruz, 1:500) and GAPDH (MAB374 Chemicon, 1:5000) were used. HDAC4 protein expression was quantified by densitometry and normalized to GAPDH protein expression using ImageQuant 5.0 software.

**Histology and immunostaining.** Mice were anesthetized with avertin and transcardially perfused first with PBS followed with 4% paraformaldehyde. Muscles were removed, immersed in 30% sucrose for cryoprotection, frozen in Tissue-Tex OCT reagent and cryosectioned into 30-40  $\mu\text{m}$ -thick longitudinal sections. Before immunostaining, sections were washed 3 x 10 minutes with PBS and blocked (5% normal goat serum, 2% BSA and 0.1% TritonX-100 in PBS) for 1hr. The sections were then incubated with Alexa488-conjugated Bungarotoxin (BTX) (A488-BTX; Invitrogen), anti-synaptotagmin-2 (ZNP-1; Developmental Hybridoma Bank (University of Iowa; Iowa City, IA)), and anti-neurofilament (SMI312; Covance) diluted in blocking solution and incubated overnight at 4 degrees. The sections were then washed 3 x 10 minutes and incubated with fluorescently tagged secondary antibodies for 1hr at room temperature

followed by three PBS washes and coverslip in Vectashield mounting medium. All images were acquired using an FV-100 confocal microscope.

Hematoxylin and eosin (H&E) and metachromatic ATPase staining were performed using standard procedures (5). Alexa594-conjugated Wheat Germ Agglutinin (WGA) (Invitrogen) was used at a concentration of 50  $\mu\text{g/mL}$ .

**Quantification of reinnervation.** Reinnervation was quantified by examining the ventral-most part of the TA muscle. Any postsynaptic end overlapping with neurofilament and/or synaptotagmin-2 was considered either partially or fully reinnervated. To quantify pre- and postsynaptic overlap, thin serial sections were collected and maximally projected using Metamorph software. The presynaptic area (labeled with synaptotagmin-2) was first traced and superimposed on the postsynaptic area (visualized using fluorescent bungarotoxin to label AChRs). The percentage of presynaptic occupancy for each junction was determined and pooled to determine pre- and postsynaptic overlap for each animal examined. All analyses and quantification of reinnervation were done blinded to the genotype. At least 200 NMJs were examined per animal.

**Motor neuron culture.** Chicken motoneurons were purified at embryonic day 5.5 as previously described (6). Factors (2 nM FGF10 and 25 ng/mL FGFBP-1) were added 3 hours after culture and incubated for 48 hours. Motoneurons were fixed and stained with anti-synapsin and acetylated-tubulin. The synapsin puncta, representing nascent synaptic

sites, were counted on an epifluorescence microscope (Zeiss). High magnification images were obtained using an Olympus FV1000 microscope.

**DNA injection into neonatal muscle.** Newborn pups were anesthetized on ice for 1-2 minutes. Using a pico-injector (Harvard Apparatus, PLI-100) and a pulled-pipette tip, cDNA (4-8  $\mu\text{g}$  in 2-3  $\mu\text{L}$  of TE buffer) was injected near the endplate band of the tibialis anterior muscle at P0. For each experiment, one leg was injected with FGFBP1 shRNA and the other with LacZ shRNA. Mice were sacrificed at P8 and the neuromuscular junctions visualized using 40  $\mu\text{m}$  cryosections as described above. 3-D imaging was used to match neuromuscular junctions with GFP-positive fibers.

**Statistical analysis.** Statistical significance was determined using an Unpaired *t* test (Graphpad). P values < 0.05 were considered to be statistically significant. All error bars represent  $\pm$  SEM. N.S. denotes  $p > 0.05$ .

## Supporting Figure Legends

### **Figure S1. Upregulation of miR-206 in symptomatic G93A-SOD1 mice.**

(A) Heat map showing miRNAs dysregulated (>2-fold) in the TA muscle of symptomatic G93A-SOD1 and wild-type (WT) littermates.

(B) Northern blot analysis of miR-206 in wild-type (WT) and G93A-SOD1 mice at the indicated ages shows up-regulation of miR-206 in symptomatic G93A-SOD1 mice.

### **Figure S2. Expression of miR-206 in adult mouse tissues.**

(A) Northern blot analysis of miR-206 expression in adult mouse tissues. U6 was used as a loading control.

(B) Transcripts for *MyoD* and *Murf1* were detected by real time PCR in TA muscles ten days after nerve transection. n=3-4 per group.

### **Figure S3. Identification of the miR-206 denervation-responsive enhancer.**

(A) Sequence alignment of the three conserved E-boxes in the miR-206 upstream region.

(B) Electrophoretic mobility shift assays demonstrate direct binding of MyoD/E12 to the three conserved E-boxes. Unlabeled wild-type (WT) oligonucleotides compete for binding, but mutant (Mt) E-box oligonucleotides do not compete. The region of the gel with the shifted probe is shown. (-) refers to extract containing protein lysate from untransfected cells.

(C) Denervation of transgenic mice containing a transgene with the hsp68 basal promoter controlling lacZ expression shows minimal  $\beta$ -galactosidase activity. Lower panels show transverse sections of muscle. Scale bar =200  $\mu$ m.



**Figure S4. Generation of miR-206<sup>-/-</sup> mice.**

(A) Targeting strategy to delete miR-206 from the *miR-206/133b* locus by replacing the pre-miR-206 sequence with a neomycin cassette flanked by loxP sites. Positions of probes used for Southern blots are shown.

(B) Southern blot analysis of genomic DNA from wild-type and heterozygous mice using an external 5' probe. Genomic DNA was digested with BamHI.

(C) Hematoxylin and eosin (H&E) and metachromatic ATPase staining show no difference in the skeletal muscle architecture and distribution of Type I (dark blue) and Type II (light blue) skeletal myofibers in the soleus muscles of wild-type (WT) and miR-206<sup>-/-</sup> (KO) mice. Scale bar=200 μm.

(D) Detection of miRNA transcripts in soleus muscles of wild type (+/+) or miR-206 mutant mice (+/- and -/-) after 5 weeks of denervation using RT-PCR. Contra-lateral leg muscle was used as control. Actin was used as a loading control. Reactions with no reverse transcriptase (-RT) were a negative control for the assay. (H<sub>2</sub>O) refers to PCR performed without the addition of cDNA.

**Figure S5. Synapse-enriched expression of miR-206.**

(A) Schematic of the *miR-206/133b* locus with positions of primers used for real time PCR to detect synaptically enriched miR-206 transcripts. The 7H4 transcript previously described is shown.

(B) Detection of miR-206 and 7H4 transcripts using RT-PCR demonstrates miR-206 sequences are part of the 7H4 transcript.

**Figure S6. Normal NMJ development in miR-206<sup>-/-</sup> mice.**

(A) NMJ development of miR-206<sup>-/-</sup> mice (KO) is similar to wild type (WT) mice at postnatal days (P) 0, 21, and 63. Thick longitudinal sections of the NMJ from WT and miR-206<sup>-/-</sup> TA muscle were co-stained with  $\alpha$ -bungarotoxin (BTX) to visualize the post-synaptic acetylcholine receptor (AChR) (red), anti-synaptotagmin (ZNP) to detect pre-synaptic vesicles (green), and anti-neurofilament (NF) to detect nerve axons (blue). Scale bar=10  $\mu$ m. n=3 for each genotype and time point.

**Figure S7. miR-206 does not regulate muscle atrophy.**

(A) H&E staining shows no difference in muscle atrophy in response to denervation in the TA muscles of wild-type (WT) and miR-206 KO mice. Scale bar= 100  $\mu$ m.

(B) Quantification of the relative amount of atrophy in G/P muscles of wild-type and miR-206 mutant (KO) mice following 3 weeks of denervation. n=7 for each genotype.

**Figure S8. Delayed presynaptic differentiation but normal axon regeneration in miR-206<sup>-/-</sup> mice.**

(A) Percentage of NMJs either fully innervated (red), partially innervated (green), or denervated (blue) after cutting the sciatic nerve in WT and miR-206 KO mice for the indicated number of weeks. n=2-6 for each genotype and time point

(B) Percentage of NMJs fully innervated (red), partially innervated (green), or denervated (blue) after crushing the sciatic nerve in WT and miR-206<sup>-/-</sup> (KO) mice for the indicated number of days. n=3-5 for each genotype and time point.

(C) Transverse sections of sciatic nerves show similar numbers of axons proximal to the muscle entry point in miR-206<sup>-/-</sup> (KO) and WT mice 3 weeks after sciatic nerve transection. Nerve fibers were labeled with an antibody to neurofilament (NF). Scale bar =10 μm.

**Figure S9. Altered gene expression in the HDAC4 pathway in miR-206<sup>-/-</sup> mice.**

(A) Schematic diagram of the *Hdac4* 3' UTR with sequence homologies of predicted miR-206 binding sites.

(B) Western blot analysis showing increased HDAC4 expression in muscle lysates isolated from wild-type (WT) and miR-206<sup>-/-</sup> (KO) mice following 3 weeks of denervation. (Ctrl.) refers to protein lysate from mice with skeletal muscle deletion of HDAC4. GAPDH protein was detected as a control. Relative expression of HDAC4 protein compared to WT lysate is indicated below.

(C) Transcripts of *Hdac4* were detected in wild-type (WT) and miR-206<sup>-/-</sup> (KO) muscles after 3 weeks of denervation. n=3-5 per group.

(D) Transcripts of *Dach2* were decreased in miR-206<sup>-/-</sup> (KO) TA muscles after 3 weeks of denervation. n=3-5 per group. \*p < 0.001

(E) Transcripts of *myogenin* were increased in miR-206<sup>-/-</sup> (KO) TA muscles after 3 weeks of denervation. n=3-5 per group.

(F) Model describing the interactions of miR-206 with the HDAC4/Dach2/myogenin pathway. The observed changes in gene expression in the pathway are consistent with miR-206 regulating HDAC4.

**Figure S10. Normal NMJ development and accelerated presynaptic differentiation in HDAC4 mKO mice.**

(A) NMJ development in HDAC4 mutant (mKO) mice is similar to wild type (WT) mice at postnatal day (P) 71. Thick longitudinal sections from WT and HDAC4 mKO TA muscle were co-stained with  $\alpha$ -bungarotoxin (BTX) to visualize the post-synaptic acetylcholine receptor (AChR) (red), anti-synaptotagmin (ZNP) to detect pre-synaptic vesicles (green), and anti-neurofilament (NF) to detect nerve axons (blue). Scale bar=10  $\mu$ m.

(B) Percentage of NMJs fully innervated (red), partially innervated (green), or denervated (blue) after crushing the sciatic nerve in WT and HDAC4 mKO mice for 7 days. n=3-8 for each genotype and time point.

(C) Percentage of NMJs fully innervated (red), partially innervated (green), or denervated (blue) after cutting the sciatic nerve in WT and HDAC4 mKO mice for 3 weeks. n=3 for each genotype and time point.

**Figure S11. Expression of secreted retrograde factors in miR-206 mutant mice.**

(A) Transcripts of candidate secreted retrograde factors were detected in miR-206<sup>-/-</sup> muscles 3-weeks after sciatic nerve transection. Expression was normalized to wild-type muscle following sciatic nerve transection. n=3-5 per group.

(B) Validation of FGFBP1 knock-down in cultured cells. Co-transfection of plasmids expressing mCherry-FGFBP1 (red) and GFP-shRNA (green) directed against *Fgfbp1* or *lacZ* demonstrates a loss of mCherry expression in GFP-expressing cells. Scale bar= 10  $\mu$ m.

**Video S1. Acceleration of ALS pathogenesis in miR-206<sup>-/-</sup> mice.**

Video of G93A-SOD1 mouse at 7 months of age.

**Video S2. Acceleration of ALS pathogenesis in miR-206<sup>-/-</sup> mice.**

Video of miR-206<sup>-/-</sup>;G93A-SOD1 littermate at 7 months of age demonstrating an acceleration of disease pathogenesis.

## Table S1. Primer Sequences

### miR-206 targeting vector (5'-3'):

5' Arm For- CCTGATGCTTCTCAATACCCTTGCTTC  
5' Arm Rev- GTAACATGTGGAGAAGCTGCTCAGCTTAG  
3' Arm For- CAAGTGCTTCTTCAAGGCCGATGG  
3' Arm Rev- TGTTCTAAGTTCCTAGGGTACACAGAGGAGACTAG  
5' Probe For- GAGGCCACTCCTCCCTGTGCTTC  
5' Probe Rev- GCAACGGGTATGAGGGTGAAGACCG  
3' Probe For- GGCCTACATCTTTCCTCTCCTTATGCCAATAC  
3' Probe Rev- GTGGGTGGGAATATACAGTAACTATGATACTGAG

### Northern probes (Starfire: 5'-3'):

miR-206- CCACACACTTCCTTACATTTCA  
miR-1- TACATACTTCTTTACATTCCA  
U6- GCAGGGGCCATGCTAATCTTCTCTGTATTG

### RT-PCR primers (5'-3'):

miR-206 For- CCCAACAAGCTCTGCCTG  
miR-206 Rev- GGGAGCATAGTTGACCTGAAAC  
miR-133b For- CTGGTCAAACGGAACCAAGT  
miR-133b Rev- TGATGGCAAACACAGCATT  
miR-1-1 For- CCTGCTTGGGACACATACTTC  
miR-1-1 Rev- CAGTCTGGCGAGAGAGTTCC  
miR-1-2 For- CATTCCATAGCACTGAATGTTTCATA  
miR-1-2 Rev- GGCTGCTTCATGTTTTTACA  
miR-133a-1 For- CATTGAAGAGGCGATTTGGT  
miR-133a-1 Rev- GAGCTGCAAGAACAGCAGTG  
miR-133a-2 For- AGCCAAATGCTTTGCTGAAG  
miR-133a-2 Rev- TGCGGCGTGATCAATG  
Dach2 For- ACTGAAAGTGGCTTTGGATAA  
Dach2 Rev- TTCAGACGCTTTTGCATTGTA  
FGFBP1 For- CTGGCTACTCAGGCGTTCTC  
FGFBP1 Rev- AAGGCAGTCAGTTGGGTCAC  
SIRPalph For- ATACGCAGACCTGAATGTGCCCAA  
SIRPalph Rev- TGGCCACTCCATGTAGGACAAGAA  
FGF7 For- ATGCGCAAATGGATACTGACACGG  
FGF7 Rev- TGCCTCGTTTGTCAATCCTCAGGT  
FGF10 For- TACTGACACATTGTGCCTCAGCCT  
FGF10 Rev- GCTTTGACGGCAACAACCTCCGATT  
FGF22 For- GCTTCTATGTGGCCATGAATCGCA  
FGF22 Rev- AGACCAAGACTGGCAGGAAGTGT  
IGF1 For- GCTGAGCTGGTGGATGCTCTTCAGTTC  
IGF1 Rev- CTTCTGAGTCTTGGGCATGTCAGTGTG  
BDNF For- ATGGGACTCTGGAGAGCGTGAA

BDNF Rev- CGCCAGCCAATTCTCTTTTTGC  
Actin For- TCATGAAGTGTGACGTTGACATCCGT  
Actin Rev- CCTAGAAGCATTGCGGTGCACGATG  
miR-206 FP-1- TTCCTTCTGCGTGACAAGTG  
miR-206 RP-1- GCCAAAACCACACACTTCCT  
miR-206 FP-2- GTGTGTGGTTTTGGCAAGTG  
miR-206 RP-2- GGGAGCATAGTTGACCTGAAA

**Gel-Shift assay oligonucleotides (5'-3') (Mutations are underlined):**

E1 WT For- AATGGCTCAACAGCTGCCAGTGTCCA  
E1 Mt. For- AATGGCTCAATCTTGGCCAGTGTCCA  
E2 WT For- GATTGTGACGCAGGTGATTGGCCACG  
E2 Mt. For- GATTGTGACGTCTTGGATTGGCCACG  
E3 WT For- TTGGAATGCTCATCTGGCAGCTGCAGCCTGTCA  
E3 Mt. For- TTGGAATGCTCATCTGGTTCTTGGCAGCCTGTCA

**Cloning primers (5'-3'):**

206 Enhancer For- CCTAAGGGAGGGAAACACACACACAC  
206 Enhancer Rev- GGGTAACATGTGGAGAACTGCTCAGCT  
Hdac4 UTR For- TTAACTGCTAACTTCTTTTCTAGCACTTAAAGC  
Hdac4 UTR Rev- ATGTATCAATGCCCATAAAATACATGG  
miR-206 Plasmid For- AGGTTGCCTGGCCATAACTACGCTG  
miR-206 Plasmid Rev- CAGTGTGTTCGGTATGCTGATGTTTTTGAG

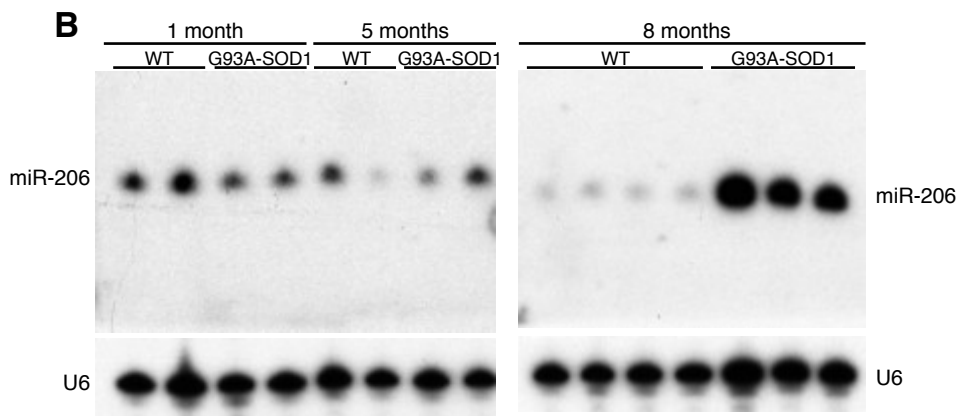
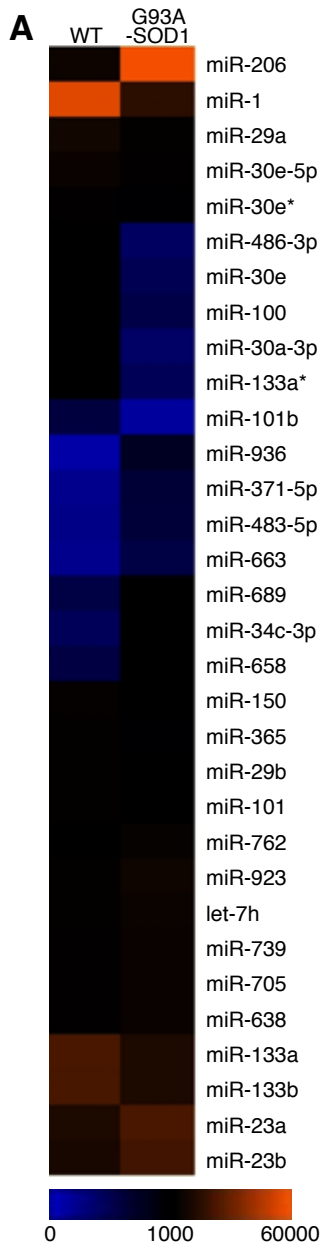
**shRNA sequences (5'-3'):**

shRNA-FGFBP1 #1-CTCATCCTGCTCTCCTTCCTT  
shRNA-FGFBP1 #2-GCTACTCAGGCGTTCTCAGAA

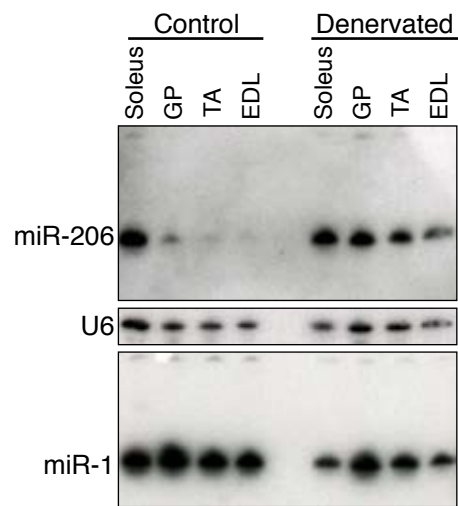
### Supporting References

1. M. J. Potthoff *et al.*, *J Clin Invest* **117**, 2459 (Sep, 2007).
2. S. Li *et al.*, *Proc Natl Acad Sci U S A* **102**, 1082 (Jan 25, 2005).
3. G. Feng *et al.*, *Neuron* **28**, 41 (Oct, 2000).
4. T. C. Cheng, M. C. Wallace, J. P. Merlie, E. N. Olson, *Science* **261**, 215 (Jul 9, 1993).
5. M. Oh *et al.*, *Mol Cell Biol* **25**, 6629 (Aug, 2005).
6. M. A. Fox *et al.*, *Cell* **129**, 179 (Apr 6, 2007).

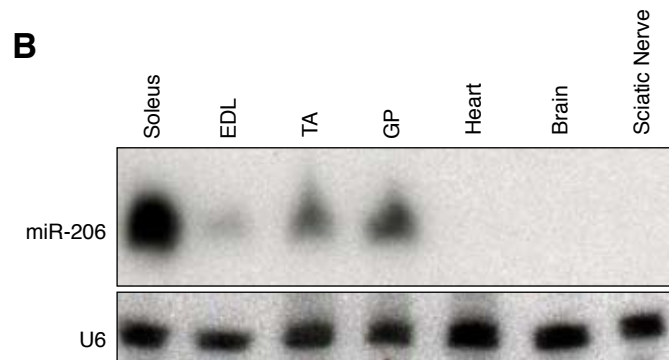
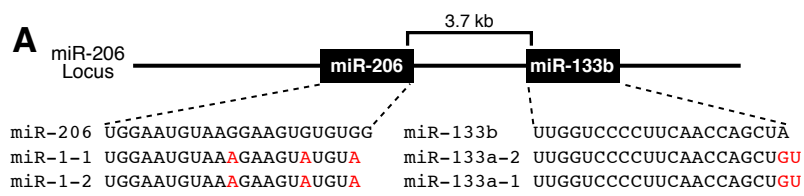


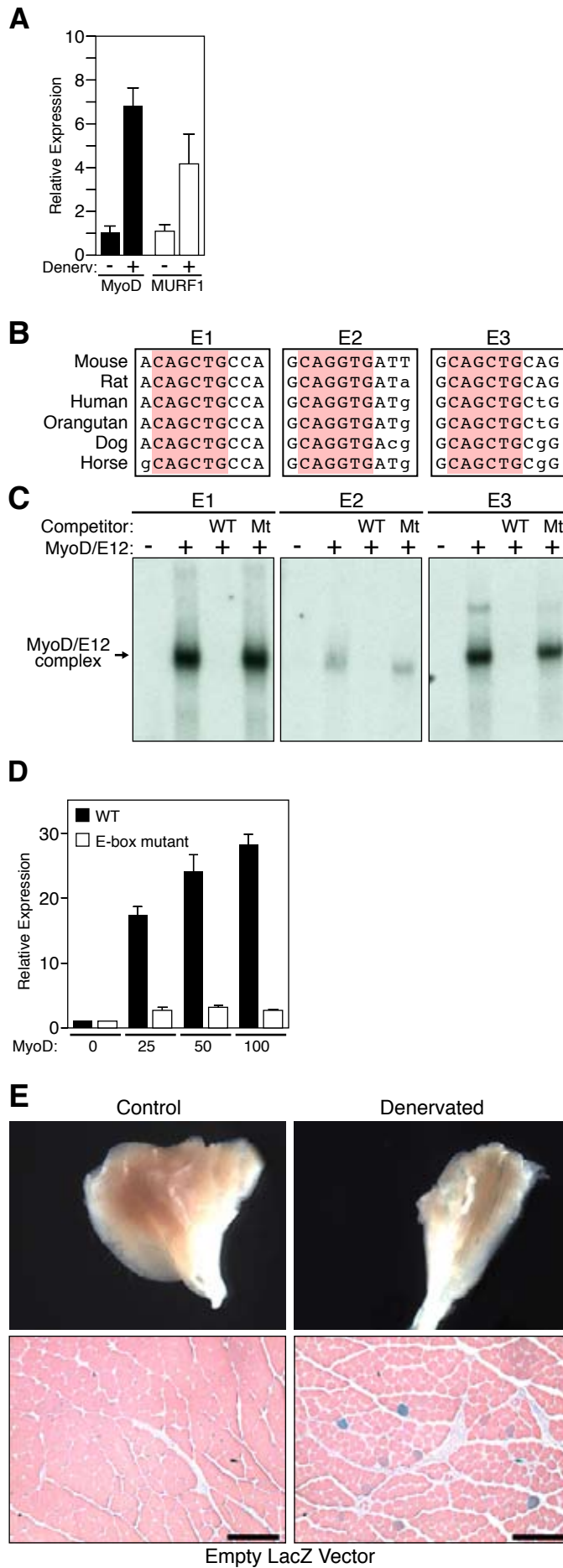


Sup. Fig. 1

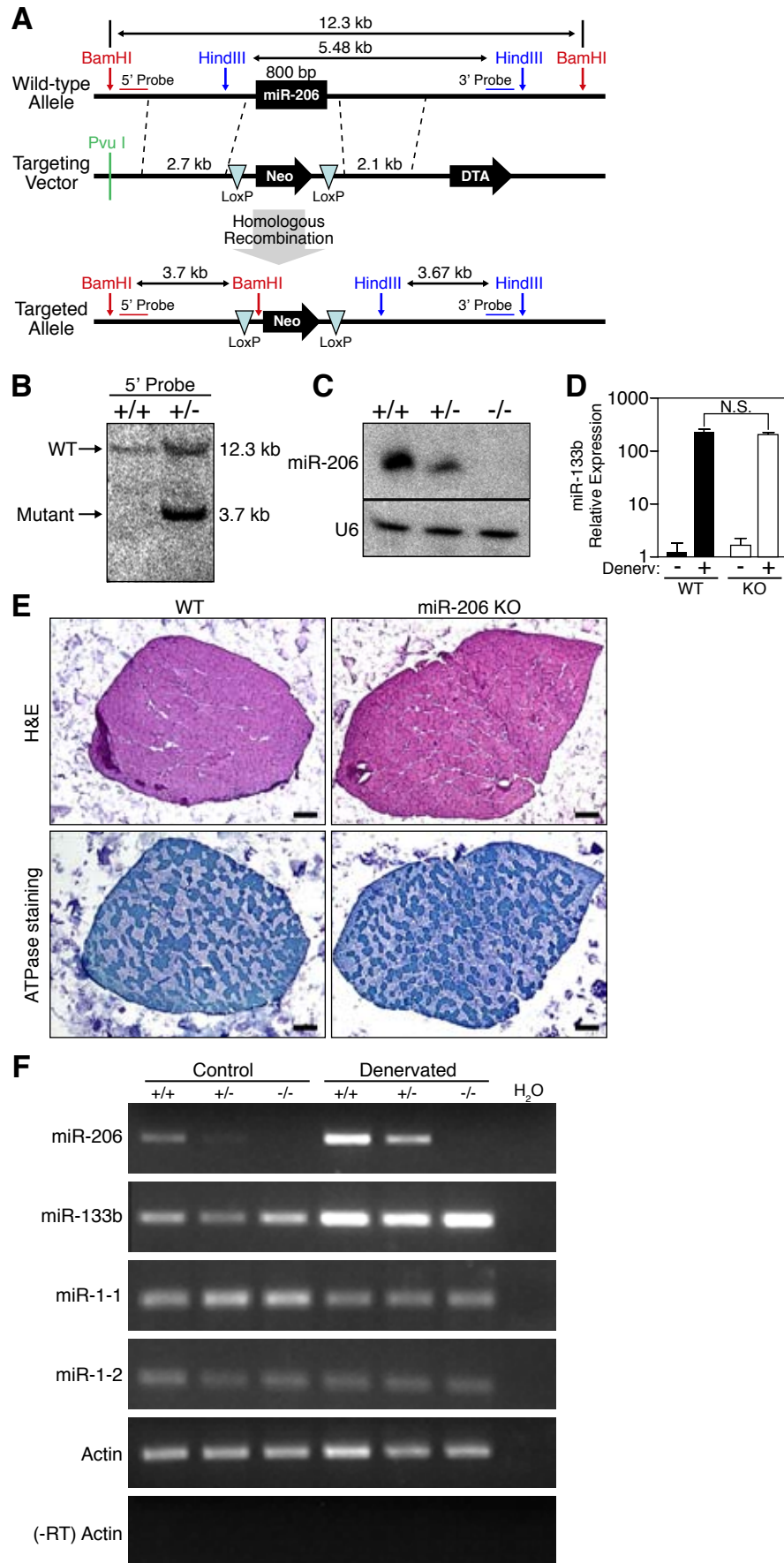


**Sup. Fig. 2**

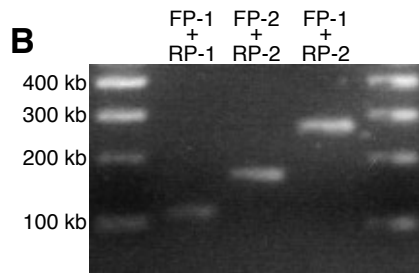
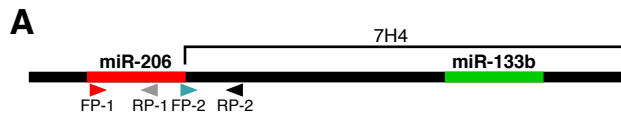


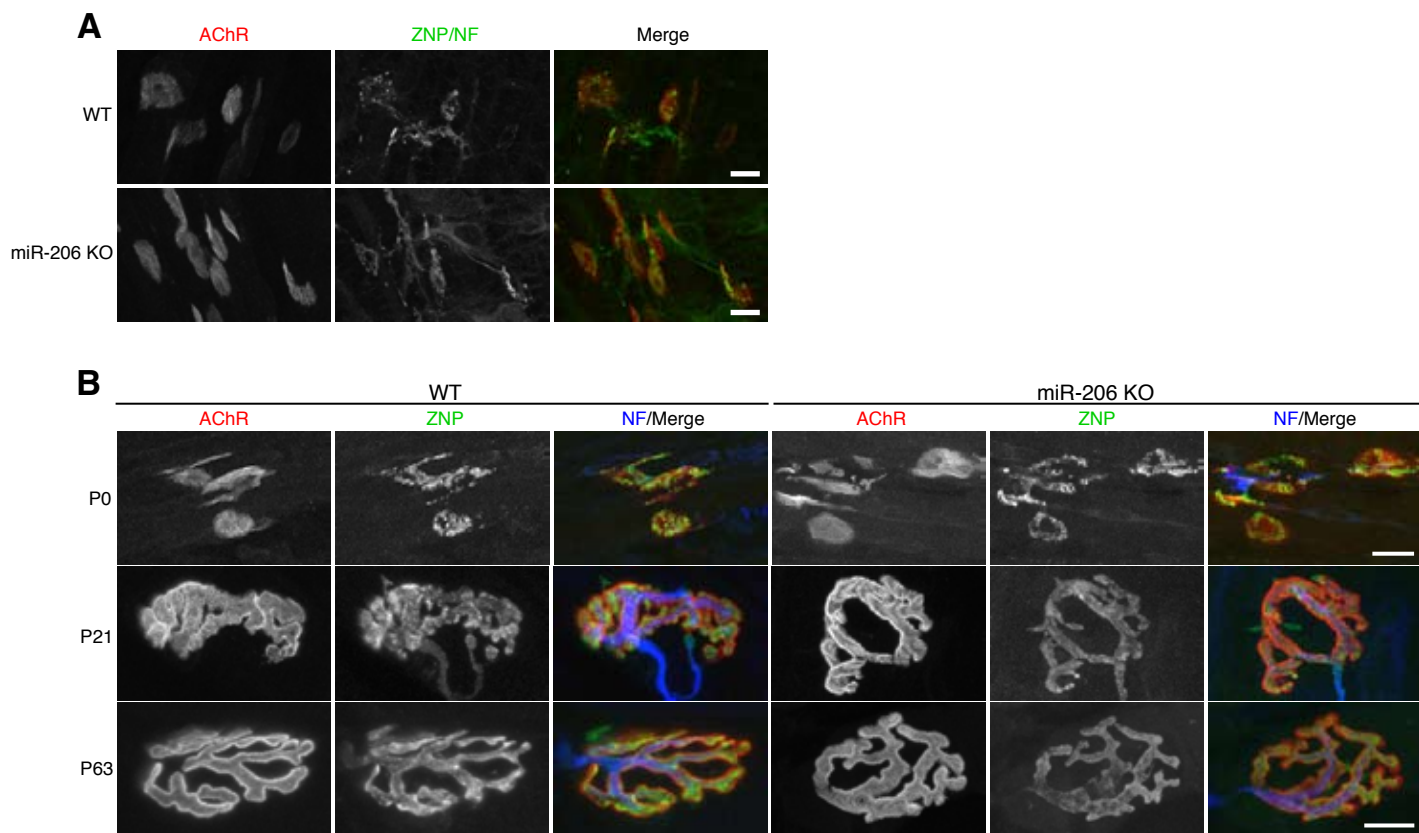


Sup. Fig. 4

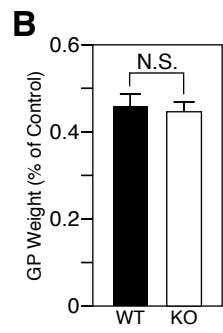
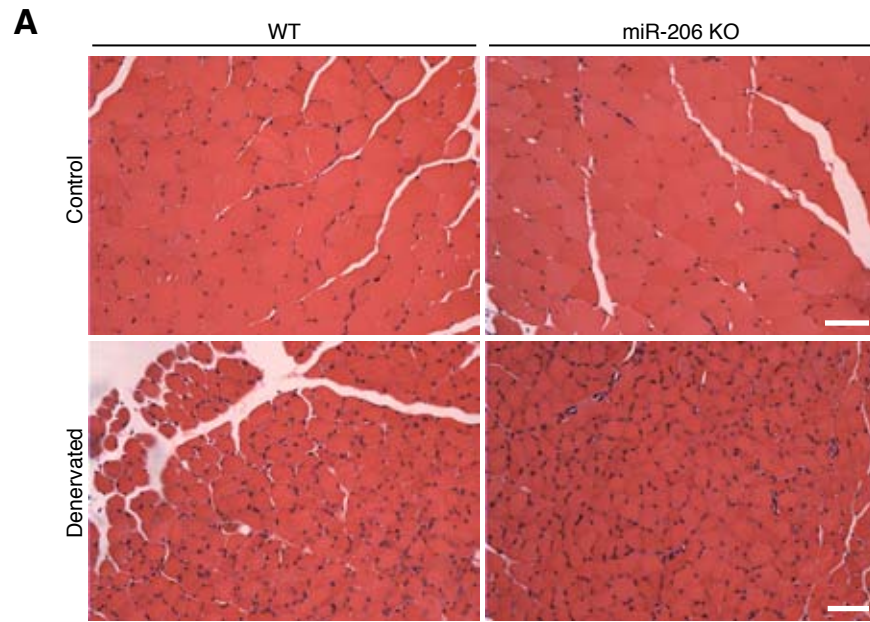


Sup. Fig. 5

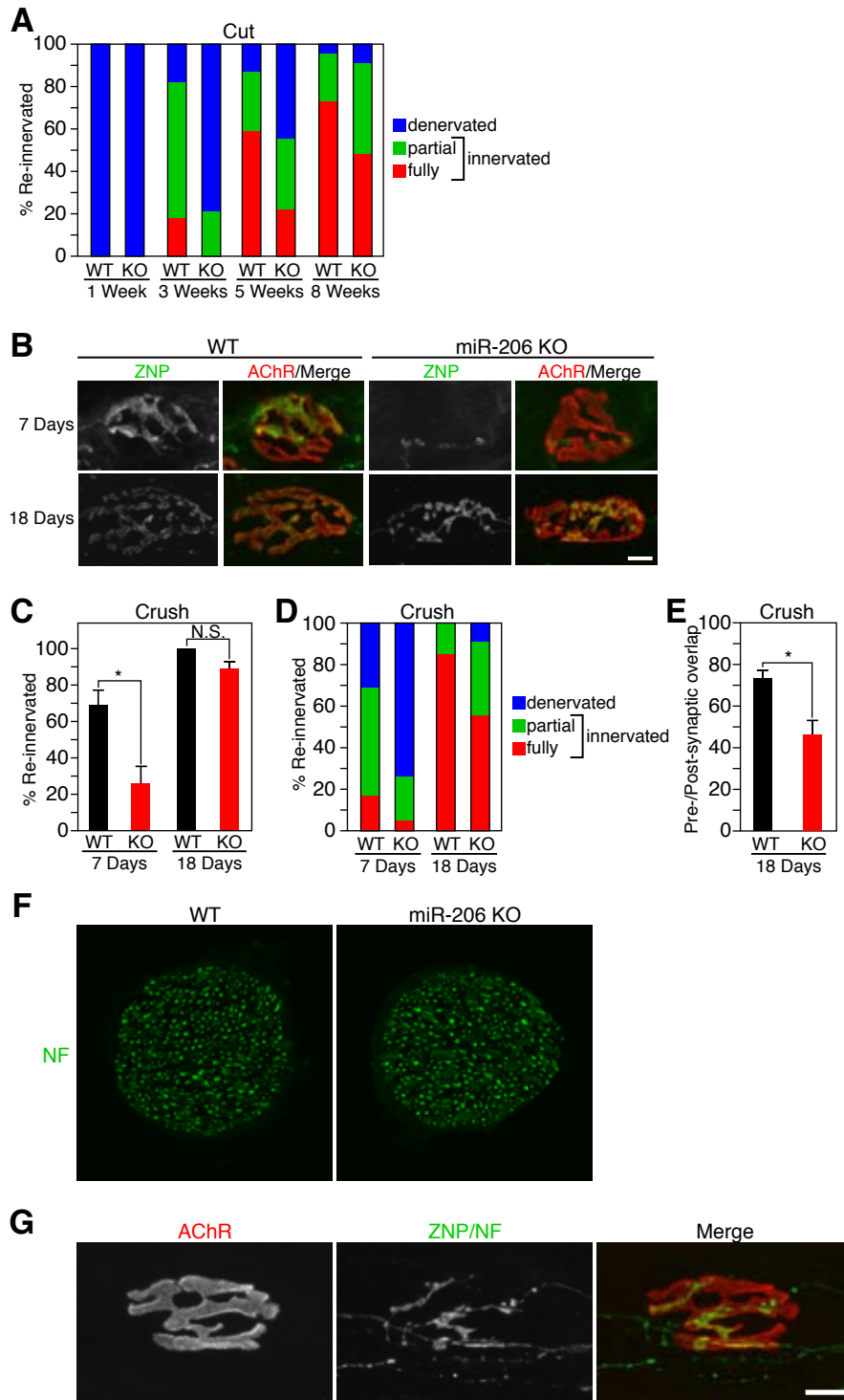




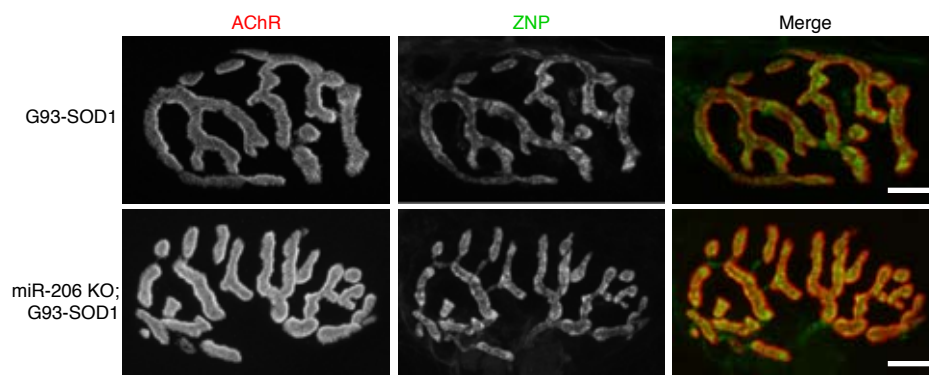
Sup. Fig. 7



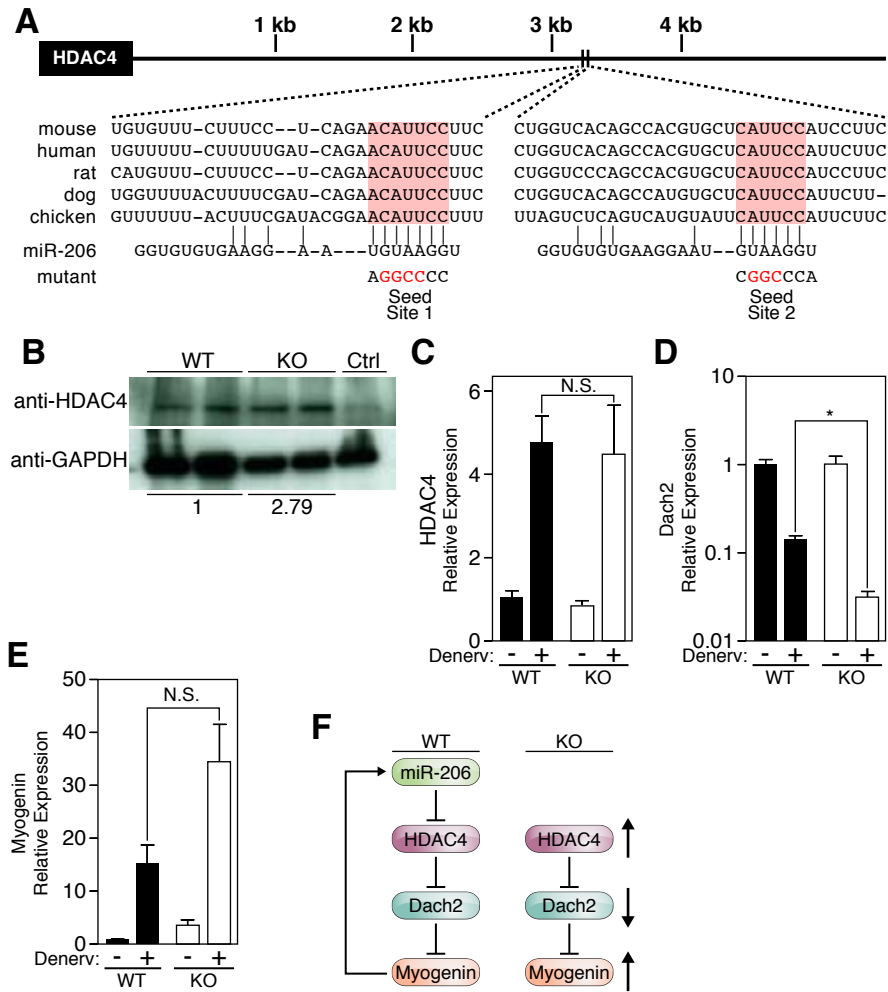


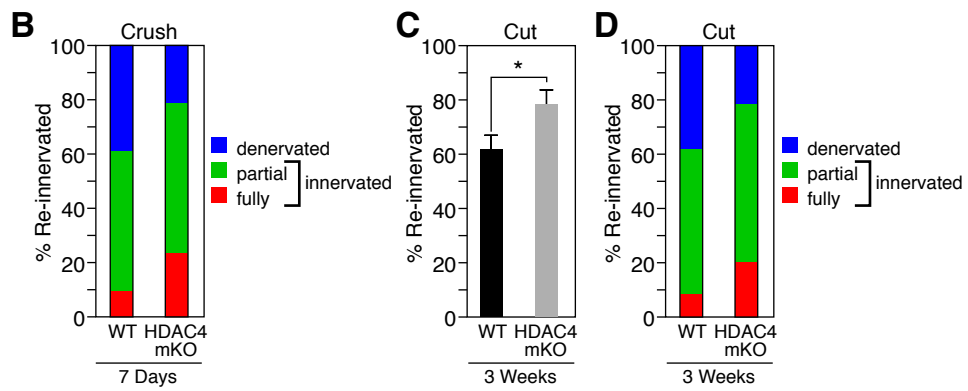
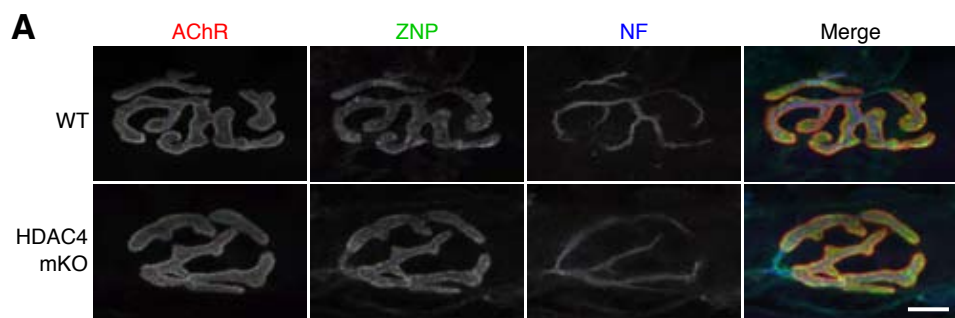


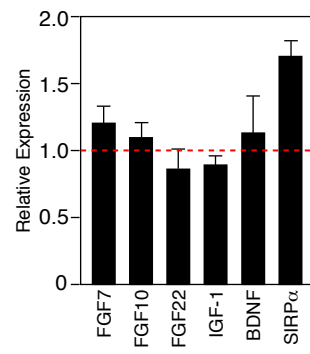
Sup. Fig. 9



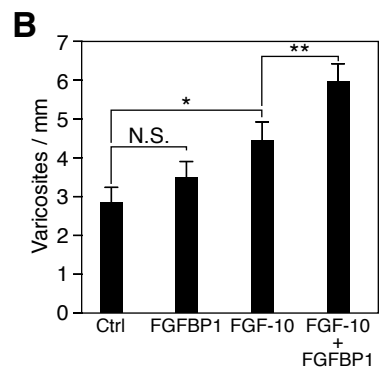
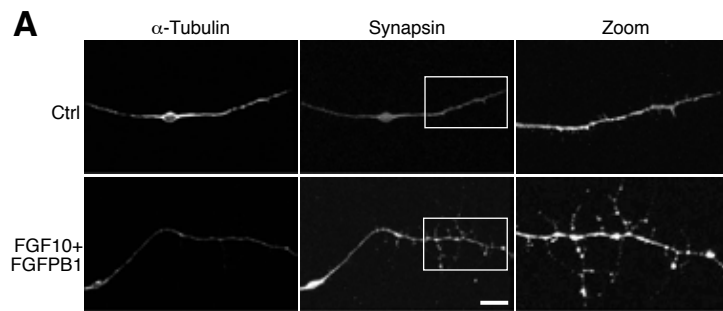
Sup. Fig. 10

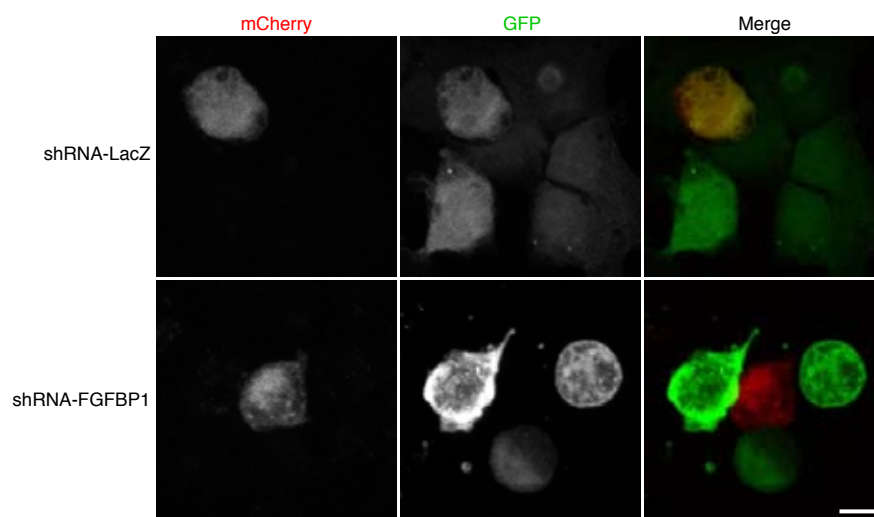






**Sup. Fig. 13**





Sup. Fig. 15